Effect of temperature on noninvasive blood glucose monitoring *in vivo* using optical coherence tomography

Ya Su (苏 亚)[1], X. Steve Yao (姚晓天)[1,4*] Zhuo Meng (孟 卓)[1,2], Longzhi Wang (王龙志)[1,3], Haimin Yu (于海民)[2], and Tiegen Liu (刘铁根)[1]

[1]*Polarization Research Center, College of Precision Instrument & Opto-electronics Engineering and Key Laboratory of Opto-electronics Information and Technical Science, Ministry of Education, Tianjin University, Tianjin 300072, China*

[2]*Suzhou Opto-ring Co. Ltd., Suzhou 215123, China*

[3]*College of Automobile and Transportation, Tianjin University of Technology and Education, Tianjin 300222, China*

[4]*General Photonics Corporation, 5228 Edison Avenue, Chino, California 91710, USA*

[*]*Corresponding author: steveyao888@yahoo.com*

Received March 12, 2014; accepted August 8, 2014; posted online October 27, 2014

Noninvasive glucose monitoring (NIGM) techniques based on optical coherence tomography (OCT) are affected by several perturbing factors, including variation of tissue temperature. We first design a temperature control module integrated with an optical scanning probe to precisely control the temperature of skin tissues. We investigate the influence of temperature on NIGM with OCT by correlation analysis at different depths of *in vivo* human skin. On average, the relative changes in attenuation coefficient (μ_t) per 1 °C of temperature lead to 0.30 ± 0.097 mmol/L prediction error of blood glucose concentration. For improving the accuracy of NIGM, this temperature dependence must be taken into account.

OCIS codes: 170.1470, 290.1350, 170.4500.
doi: 10.3788/COL201412.111701.

Diabetes mellitus can cause some complications such as cardiovascular and cerebrovascular disease, renal failure, diabetic retinopathy, and nerve damage[1]. For most patients, the current glucose sensing techniques are still invasive methods which not only cause pain to individuals but are also coupled with possibility of infection. Therefore, noninvasive methods have been thought to be an attractive alternative. Several teams conducted research in this field and several techniques such as microwave spectrum[2], near-infrared[3,4] and mid-infrared spectroscopy[5], Raman spectroscopy[6], fluorescence[7], optical polarimetry[8], optoacoustic technique[9,10], and optical coherence tomography (OCT)[11] have been under investigation in the past years.

OCT is a high-resolution imaging technique and can be applied to noninvasive glucose monitoring (NIGM)[12–14]. The variations of the blood glucose concentration (BGC) can induce changes in μ_t at certain depth regions of biological tissues. Therefore, one can measure BGC by analyzing the glucose-induced changes in μ_t detected in such regions. Most of the noninvasive methods that detect BGC need to be operated in well-controlled conditions, because there are many complicated factors that can influence the optical properties in tissues[15–18]. Temperature is one of the important parameters that can affect noninvasive blood glucose measurement. However, there are few studies on the effect of temperature on NIGM with OCT quantitatively.

In this letter, we show *in vivo* studies using OCT to analyze the effect of temperature variation on NIGM. We present accurate measurement results of temperature- and glucose-induced changes in μ_t of human skin. The OCT signals are acquired from the volar side of forearm skin, while temperature and glucose are experimentally varied within their physiological ranges.

A schematic diagram of the OCT system and temperature-controlled optical probe is shown in Fig. 1. The light source that has 1325 nm central wavelength is built in the swept source OCT system. The imaging depth of the system is 3 mm. The axial resolution and transverse resolution are 12 and 25 μm, respectively. A three-dimensional (3D) image with dimensions of 152×152×512 pixel size is obtained in 8 s. Each A-scan consists of 512 pixels in depth (Z) direction. The size of the image is 3.75×3.75×3 (mm) (X×Y×Z).

The skin temperature is monitored using a small temperature sensor attached on the skin surface adjacent to the OCT imaged 3D area. The temperature controller that can real-timely adjust its output power drives the thermo-electric component (TEC) according

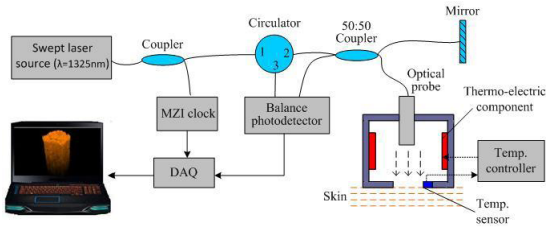

Fig. 1. Schematic of the temperature-controlled optical system consisting of a swept source OCT, a TEC, and a temperature controller.

to a feedback temperature from the sensor. The TEC can either heat or cool air in the sealed thermostat to vary the temperature of skin tissues.

The skin surface of the 3D OCT image (Fig. 2(a)) is first detected by an image identification algorithm. Then all A-scans of the OCT image are realigned to flatten the surface and thereby a 3D image is reconstructed. Subsequently, all A-scans of the reconstructed OCT volume are averaged to have a one-dimensional (1D) signal (Fig. 2(b)) to suppress the speckle noise and minimize motion artifacts so as to improve the measurement precision of tissue optical properties[19].

OCT can be used for quantitative analysis of tissue optical properties along with imaging. For homogeneous, non-absorbing media, the light intensity of ballistic photons obeys the Beer–Lambert law

$$I = I_0 e^{-\mu_t z}, \tag{1}$$

where $\mu_t = \mu_s + \mu_a$ is the attenuation coefficient, I_0 is the incident light intensity, z is the geometric depth inside the tissue, and μ_s and μ_a are the scattering and absorption coefficients, respectively. For a strongly scattering material in the near-infrared spectral range, μ_s is much greater than μ_a and μ_t can be replaced with μ_s. Therefore, one can measure μ_s by analyzing the slope value of the linear fitting on the OCT signal in a specified depth of region.

Figure 2(b) shows that an intensity profile of the averaged A-scan has two maximum peaks, which is caused by the two bright reflecting bands. Skin surface is the first maximum peak. The epidermis is between the surface and the local intensity minimum. The second peak is caused by the reflection of dermal fibers. The layer between the first minimum and the second maximum peaks corresponds to the junction of epidermis and the upper dermis, papillary layer. Thus, the border of the dermis is characterized by the second maximum peak[20,21].

Nine normal healthy human subjects (aged between 24 and 33 years) were considered for the study and divided into two groups. The OCT signals were obtained from the volar side of the forearm skin. During the measurement, each volunteer was asked to remain still to minimize motion artifacts. Furthermore, we placed thin fiducial marker on the skin of the subject and used edge feature extraction technique in image acquisition. The feature-based method provided for consistency of detected region of skin and corrected the error caused by motion artifact[22].

We performed two sets of experiments. In the first experiment, we investigated repetition and consistency of the temperature dependence of μ_t for human skin in four human subjects. Their BGC were stable during the experiments. The temperature was modulated periodically in the physiological range from 31 to 39 °C in three cycles. In the second experiment, we examined the effects of BGC and temperature on μ_t of human skin. Standard oral glucose tolerance test (OGTT) using 75 g of glucose was performed in five human subjects. Whole-blood samples were drawn from the subjects' fingertips. In order to avoid the effect of skin pressure on optical properties of tissue caused by OCT probe in multi-measurement, we performed OGTT and temperature modulation in one experiment to prevent the effect of pressure variations.

The living human skin has complex composition of tissue in several distinctive layers with various thicknesses. These tissues have their own optical characteristics. Furthermore, a distribution of these tissues in each layer is also nonuniform with depth. Different tissues have different temperature or glucose dependencies of optical properties. Thus, the correlation between μ_t and temperature or glucose is varied at different depths of human skin. In order to investigate the effect of temperature and glucose on μ_t of these tissues, it is essential to first use correlation analysis to find the maximum correlation region containing minimum noise interference. We calculated the dependence of μ_t versus temperature and glucose for the segments with a step of 25 μm (overlapped segments) in the dermis layer by a correlation analysis algorithm[23]. According

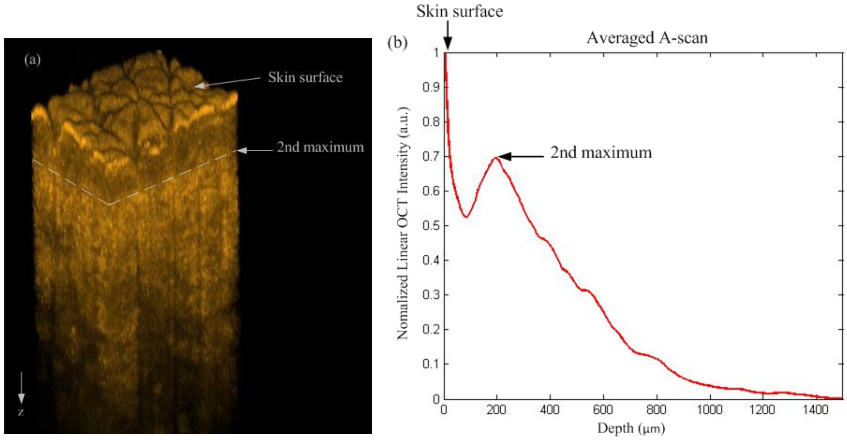

Fig. 2(a) 3D OCT image obtained from the volar side of forearm skin. (b) 1D normalized distribution of light intensity versus depth averaged by all A-scans in one reconstructed OCT 3D image from (a).

to the correlation analysis, the correlation coefficient (R) between μ_t and temperature or glucose at different depth regions can be acquired.

Figure 3 shows an effect of temperature modulation on μ_t in human skin *in vivo*. The skin temperature is changed periodically between 31 and 39 °C in three cycles. The μ_t changes back and forth with temperature and has similar value of each degree in the temperature circles. The experimental results are consistent with those in Refs. [24–26]. For subject 1, the strongest correlation (R = 0.977) between μ_t and temperature is found at the depth of 200–450 μm including the junction of papillary layer and reticular layer. For subject 2, a strong correlation (R = 0.951) is observed at the depth of 550–775 μm. This layer corresponds to the reticular layer in dermis. For subjects 3 and 4, the attenuation coefficients are calculated at the depth of 500–700 μm (R = 0.989) and 600–850 μm (R = 0.935), respectively. The temperature-dependent μ_t may be due to the structural changes in the fibers with temperature variation so that it might have an influence on the angular dependence of scattering properties[24].

Skin has a nonuniform distribution of vasculature with depth. The capillaries and venous plexus are concentrated in the dermis layer. During heat exposure, increase in skin temperature triggers cutaneous vasodilation. On the other hand, decrease in skin temperature causes cutaneous vasoconstriction[27]. Thus, the blood vessel volume can be changed by varying the temperature, which leads to refractive index mismatch with its surrounding medium, and thus affects the tissue optical properties.

The results of the second set of experiment are summarized in Table 1. It can be clearly seen that the changes in μ_t caused by 1 °C of temperature variation are much less than the changes caused by 1 mmol/L of BGC variation for all the subjects. The relative changes in μ_t induced by 1 mmol/L changes of BGC ranged from 2.3 to 4.7 times than changes in μ_t associated with 1 °C of temperature variation, with a mean of 3.5 ± 0.9 times for the five subjects investigated. Thus, moderate skin temperature fluctuations in the range of ±1 °C do not substantially degrade the accuracy of BGC prediction using OCT; however, substantial skin heating

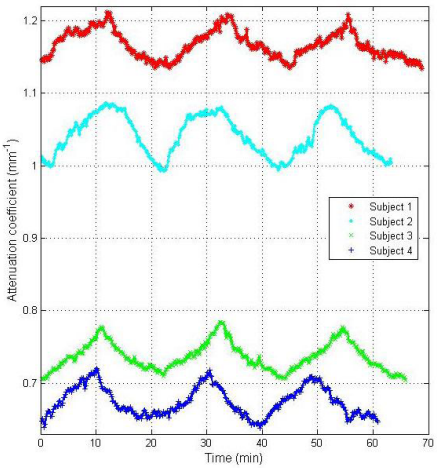

Fig. 3. Effect of temperature modulation on μ_t of the forearm skin of four subjects in the first experiment. Skin temperature cycling was modulated periodically between 31 and 39 °C in three cycles within 70 min.

or cooling (several degree) will significantly change μ_t and therefore degrade the associated BGC prediction. The result is similar to that reported for the effect of temperature on the skin of rabbit ear *in vivo*[18].

Figure 4 illustrates typical result of experiment on reproducibility of μ_t, corresponding BGC and temperature modulation over time in subject 1. The μ_t is calculated at the depth of 400–700 μm in dermis layer of forearm area. The R of μ_t with BGC is 0.865. After drinking 75 g of glucose solution within 36 min, the BGC of subject 1 increases up to 8.0 mmol/L and the temperature of skin is maintained at 31.8 ± 0.2 °C in this period. Thus, the changes in μ_t is mainly induced by variation of BGC at this stage. We use the least-square fit to analyze the changes in μ_t with BGC and the fitted slope is regarded as BGC coefficient. The BGC coefficient of μ_t is 0.0152 mm^{-1}/mmol/L (Fig. 5(a)). In the next 37 to 150 min, the BGC begins to decrease and temperature modulation is performed. Temperature varies between 31 and 39 °C back and forth in one circle and the circle is repeated four times. We calculate the correlation between μ_t and

Table 1. Results of the Second Experiment to Investigate the Effects of BGC and Temperature on μ_t of Human Skin

Subject No.	Calculated Depth Region (μm)	R for BGC	R for Temperature	BGC Coefficient of μ_t (mm^{-1}/mmol/L)	Temperature Coefficient of μ_t (mm^{-1}/°C)
1	400–700	0.865	0.965	0.0152	0.0066
2	225–625	0.984	0.989	0.0389	0.0083
3	400–900	0.903	0.966	0.0194	0.0048
4	200–675	0.812	0.882	0.0302	0.0091
5	300–650	0.806	0.952	0.0249	0.0075

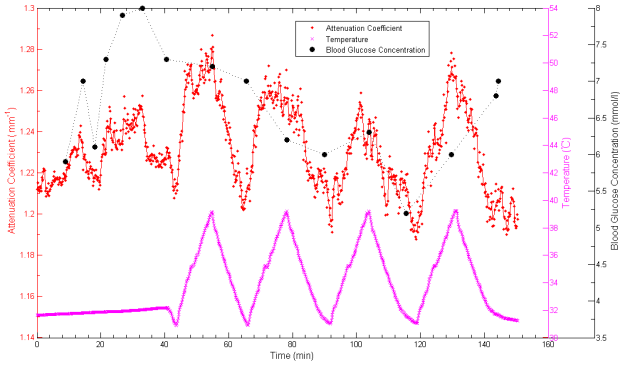

Fig. 4. Attenuation coefficient μ_t, corresponding BGC and temperature versus time in subject 1.

temperature at the stage (78–104 min) in which the BGC is stable with the range from 6.2 to 6.3 mmol/L. Therefore, the changes in μ_t is mainly induced by variation of temperature at this stage. The R value is 0.965 and the temperature coefficient is 0.0066 $mm^{-1}/°C$ (Fig. 5(b)). The relative changes in μ_t induced by 2.3 °C of temperature variation are equal to the changes induced in μ_t by 1 mmol/L changes in BGC.

Previous studies showed that the correlation between μ_t and BGC was negative at a fixed region of certain depth[11,28]. However, subsequent research indicated that the R can be positive (μ_t increased with BGC) or negative (μ_t decreased with BGC) at different depths of skin[16,17,19], which is due to the layered structure and distribution of tissues with depth of human skin. Thus, the range of R varies from −1 to +1 at different regions along the depth of skin. The results are verified by our previous study[23]. In Fig. 5, the correlation that μ_t increases with BGC is in agreement with other findings[17,19].

In OGTT experiment, the blood glucose level of human subject rises quickly after drinking 75 g glucose. In the meantime, the pancreas releases insulin into the blood to decrease BGC by moving blood sugar (glucose) into the cells of human body[29]. Thus, the BGC takes on a fluctuant increasing process. As shown in Fig. 4, there is a drop from 7.0 to 6.1 mmol/L which can be considered a fluctuation during the rising stage of BGC. The fluctuation range of BGC varies in

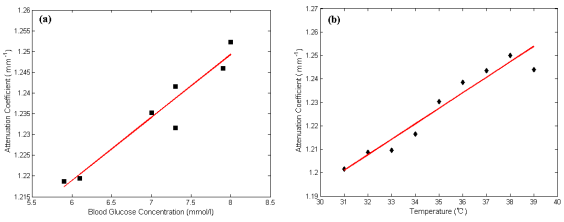

Fig. 5. Measured μ_t versus (a) BGC and (b) temperature of subject 1. The solid line is the linear least-square fitting of the experimental data. The fitted slope is regarded as (a) BGC or (b) temperature coefficient.

different subjects because of individual differences and ±1 mmol/L is in a reasonable range[30].

One possible interpretation of the glucose effect on μ_t is that the variation of glucose concentration results in the refractive index mismatch between the extracellular fluid and scattering centers and thus affects the tissue scattering properties. The second hypothesis is based on morphological changes in tissue. The collagen fibers can be swollen or shrunk with a varied BGC in the dermis layer. Therefore, the reversible shift of fibers may result in changes in the μ_t with BGC at a certain depth[17,18].

In conclusion, we investigate the effect of BGC and temperature changes in μ_t of *in vivo* human skin by OCT. The results show that there are good correlations between changes in μ_t and BGC during OGTT experiments. The μ_t is observed to change repetitively with the temperature from 31 to 39 °C. On average, the relative changes in μ_t per 1 mmol/L of BGC produce 3.5 ± 0.9 times than that induced by 1 °C of temperature variation. That is, the changes in μ_t per 1 °C of temperature lead to 0.30 ± 0.097 mmol/L prediction error of BGC. Thus, the effect of temperature on BGC prediction should be taken into account at wide temperature fluctuations of human skin. The knowledge of such thermal effect on BGC prediction can be used to improve the accuracy and reliability of measured value in NIGM.

This work was supported by the National "973" Program of China (No. 2010CB327806), the International Science & Technology Cooperation Program of China (No. 2010DFB13180), the Medical Instruments and New Medicine Program of Suzhou (No. ZXY2012026), and the Foundation Research Project of Jiangsu Province (No. BK20130374).

References

1. World Health Organization, "Health topics: diabetes: world diabetes day," http://www.who.int/mediacentre/events/annual/world_diabetes_day/en/index.html (2012).
2. J. H. Park, C. S. Kim, B. C. Choi, and K. Y. Ham, Biosens. Bioelectron. **19,** 321 (2003).
3. L. A. Nelson, J. C. McCann, A. W. Loepke, J. Wu, B. B. Dor, and C. D. Kurth, J. Biomed. Opt. **11,** 064022 (2006).
4. R. Liu, W. Chen, X. Gu, Y. Luo, and K. X. Xu, Proc. SPIE **5702,** 30 (2005).
5. S. L. Yu, D. C. Li, H. Chong, C. Y. Sun, H. X. Yu, and K. X. Xu, Biomed. Opt. Express **5,** 275 (2014).
6. A. M. Enejder, T. G. Scecina, J. Oh, M. Hunter, W. C. Shih, S. Sasic, G. L. Horowitz, and M. S. Feld, J. Biomed. Opt. **1,** 031114 (2005).
7. F. Hussain, D. J. S. Birch, and J. C. Pickup, Anal. Biochem. **339,** 137 (2005).
8. R. R. Ansari, S. Böclde, and L. Rovati, J. Biomed. Opt. **9,** 103 (2004).
9. Z. Ren, G. Liu, and Z. Huang, Chin. Opt. Lett. **11,** S21701 (2013).
10. L. Zhu, J. Lin, B. Lin, and H. Li, Chin. Opt. Lett. **11,** 021701 (2013).
11. R. O. Esenaliev, K. V. Larin, I. V. Larina, and M. Motamedi, Opt. Lett. **26,** 992 (2001).

12. R. V. Kuranov, V. V. Sapozhnikova, D. S. Prough, I. Cicenaite, and R. O. Esenaliev, J. Diabetes Sci. Technol. **1,** 470 (2007).
13. M. Kinnunen, R Myllylä, T. Jokela, and S. Vainio, Appl. Opt. **45,** 2251 (2006).
14. M. G. Ghosn, N. Sudheendran, M. Wendt, A. Glasser, V. V. Tuchin, and K. V. Larin, J. Biophoton. **3,** 25 (2010).
15. O. S. Khalil, Diabetes Technol. Therap. **6,** 660 (2004).
16. V. V. Sapozhnikova, R. V. Kuranov, I. Cicenaite, R. O. Esenaliev, and D. S. Prough, J. Biomed. Opt. **13,** 021112 (2008).
17. V. V. Sapozhnikova, D. Prough, R. V. Kuranov, I. Cicenaite, and R. O. Esenaliev, Exp. Biol. Med. **231,** 1323 (2006).
18. K. V. Larin, M. Motamedi, T. V. Ashitkov, and R. O. Esenaliev, Phys. Med. Biol. **48,** 1371 (2003).
19. R. V. Kuranov, V. V. Sapozhnikova, D. S. Prough, I. Cicenaite, and R. O. Esenaliev, Phys. Med. Biol. **51,** 3885 (2006).
20. Y. Hori and Y. Yasuno, Opt. Express **14,** 1862 (2006).
21. J. Welzel, Res. Technol. **7,** 1 (2001).
22. Y. M. Liew, R. A. McLaughlin, F. M. Wood, and D. D. Sampson, Biomed. Opt. Express **3,** 1774 (2012).
23. Y. Su, Z. Meng, L. Z. Wang, H. M. Yu, T. G. Liu, and X. T. Yao, Chin. J. Lasers **41,** 0704002 (2014).
24. J. Laufer, R. Simpson, M. Kohl, M. Essenpreis, and M. Cope, Phys. Med. Biol. **43,** 2479 (1998).
25. S. J. Yeh, O. S. Khalil, C. F. Hanna, S. Kantor, X. Wu, T. W. Jeng, and R. A. Bolt, Proc. SPIE **4250,** 455 (2001).
26. O. S. Khalil, S. J. Yeh, M. G. Lowery, X. M. Wu, C. F. Hanna, S. Kantor, T. W. Jeng, J. Kanger, R. A. Bolt, and F. F. M. de Mul, J. Biomed. Opt. **8,** 191 (2003).
27. J. Allen, J. R. Frame, and A. Murray, Physiol. Meas. **23**, 365 (2002).
28. K. V. Larin, M. S. Eledrisi, M. Motamedi, and R. O. Esenaliev, Diabetes Care **25**, 2263 (2002).
29. J. E. Grunwald, C. E. Riva, D. B. Martin, A. R. Quint, and P. A. Epstein, Ophthalmology **94**, 1614 (1987).
30. M. A. Pleitez, T. Lieblein, A. Bauer, O. Hertzberg, H. V. Lilienfeld-Toal, and W. Mäntele, Anal. Chem. **85**, 1013 (2012).